A Day-to-day Invariant Macroscopic Fundamental Diagrams for Probe Vehicles

Jingyi Hao[1] and Zhengbing He[2*]

[1]School of Traffic and Transportation, Beijing Jiaotong University, China;

[2]College of Metropolitan Transportation, Beijing University of Technology, China.

[*]Corresponding author's e-mail: he.zb@hotmail.com

Abstract. The macroscopic fundamental diagram (MFD) for an urban area provides a new thought on aggregate traffic management and control that are less affected by details. The MFD is conventionally constructed by using loop detector data, which may not widely exist due to the limited coverage of hardware installation. In contrast, the probe vehicle data have the benefits of low cost and wide coverage. To make use of the widely existing low cost data, we propose an MFD for probe vehicles (*p*MFD). Taking Beijing road network as an example, we empirically demonstrate that the *p*MFD is day-to-day invariant in shape. We then explicitly analyse the relation between the *p*MFD and the conventional MFD. This study relaxes the data constraint of the MFD construction and provides a new insight on macroscopic network condition monitoring.

1. Introduction

Recently, a macroscopic fundamental diagram (MFD) for an urban area is proposed and immediately becomes a topic that is very hot in the field of transportation research. Its major advantage is the capability of reflecting invariant macroscopic relationships among space-mean flow, density, and speed in a large urban area. It provides a new thought on aggregate traffic management and control that is less affected by details.

For the first time, Geroliminis et al (2008) provided an empirical evidence showing that a well-defined MFD exists for an urban area in Yokohama, Japan. Since then, various studies demonstrated that the MFD could be constructed using empirical data or simulation data of large-scale urban networks (Buisson and Ladier, 2009; Geroliminis and Sun, 2011; Nagle and Gayah, 2014; Saberi et al, 2013; Tsubota et al, 2014; He et al, 2014).

Although the MFD is a significant tool for transportation management (Haddad et al, 2012; Zheng et al, 2012; Keyvan-Ekbatani et al, 2012; Ramezani et al, 2015; Haddad et al, 2016; Mariotte et al, 2017), most of the research still construct the MFD using stationary detector data (SDD). Obviously, it is costly to install network-wide stationary detectors. In contrast, probe vehicle data (PVD) is cheaper and nowadays widely exists due to the prevalence of mobile sensors such as mobile phone and navigation devices. However, few studies focus on the construction of MFD based on PVD. Beibei et al (2016) investigated the MFD of Changsha, China with real data using traffic counts from SDD and traffic densities from PVD. The study found that the varied spatial distribution of the taxi proportion rate appear to be statistically significant. Ambhl et al (2016) proposed a fusion algorithm for estimating the MFD based on both SDD and PVD simultaneously. The proposed algorithm could significantly reduce the estimation error comparing with stand-alone data (i.e. SDD or PVD on their

own). Nagle and Gayah (2014) explicitly considered the uncertainties of the network variables, where the number of floating cars is assumed to be a binomial random variable. Du et al (2016) developed a method to estimate the MFD using floating cars considering varying market penetration rates under heterogeneous demands. Both of the studies attempted to estimate the overall network variables (i.e., average network flow and density) from partial PVD. Nevertheless, to estimate the probe penetration rates, SDD has to be used, i.e., they are not completely independent on SDD.

In the paper, we propose an MFD for probe vehicles (*p*MFD) in order to demonstrate aggregated network traffic conditions using less data. We first empirically show that the *p*MFD is day-to-day invariant. Then, the relationship between the conventional MFD and the *p*MFD is explicitly discussed. The rest of the paper is organized as follows: In Section 2, the method of constructing *p*MFD is introduced. Taking Beijing road network as an example, Section 3 empirically demonstrates that the *p*MFD is day-to-day invariant. Then, the shape of *p*MFD is explicitly investigated based on a network simulation model in Section 4. Finally, a conclusion is given.

2. Methodology

2.1. Conventional MFD
Let d and i be a day and a time interval, respectively. Based on the Edie's generalized definitions (Edie,1965), the average network flow and density during time interval i on day d, which is used to constructed the macroscopic fundamental diagram, can be written as

$$\bar{q}(d,i) = \frac{l(d,i)}{LT} = \frac{N(d,i) \cdot \bar{l}(d,i)}{LT} \tag{1a}$$

$$\bar{k}(d,i) = \frac{t(d,i)}{LT} = \frac{N(d,i) \cdot \bar{t}(d,i)}{LT} \tag{1b}$$

where $N(d,i)$ is total number of the vehicles traveling in the network during time interval i on day d; $l(d,i)$ and $\bar{l}(d,i)$ are total and average distance traveled by those vehicles, respectively; $t(d,i)$ and $\bar{t}(d,i)$ are total and average time spent by those vehicles, respectively; T is the identical length of time intervals during a day, and L is the total length of all roads in the network.

2.2. MFD for probe vehicles
Define a ratio of the number of probe vehicles to the number of all vehicles during time interval i on day d as follows

$$\delta(d,i) = \frac{N_P(d,i)}{N(d,i)} \tag{2}$$

where $N_P(d,i)$ is the number of probe vehicles.

We make the following assumptions：

(i) The ratio $\delta(d,i)$ in the same time interval of different days are approximately equal, i.e.,

$$\delta(d,i) \approx \delta(d+j,i) \tag{3}$$

where $j \neq 0$ and $j \epsilon R$. According to the assumption and for simplicity, we replace $\delta(d,i)$ with $\delta(i)$ hereafter.

(ii) Denote by $\bar{l}_p(d,i)$ and $\bar{t}_p(d,i)$ the average time (i.e., vehicle kilometer traveled, VKT) and distance traveled (i.e., vehicle hour traveled, VHT) by probe vehicles, respectively, and they are approximately equal to the ones traveled by all vehicles, i.e.,

$$\bar{l}_p(d,i) \approx \bar{l}(d,i) \tag{4a}$$

$$\bar{t}_p(d,i) \approx \bar{t}(d,i) \tag{4b}$$

The assumptions are reasonable. If we take taxicabs that usually play the role of probe vehicles as an example, the number of taxicabs during the same time interval on different days are approximately equal; i.e., $N_P(d,i) \approx N_P(d+j,i)$. Similarly, according to the similarity shown by the traffic demands on multiple days, we may reasonably assume that $N(d,i) \approx N(d+j,i)$. It is also understandable that within a large road network the more the probe vehicles the more all other vehicles. Then, we could give the assumption (i). Moreover, the total number of vehicles in a network

is large, and probe vehicles with a certain proportion of all vehicles are capable of representing all vehicles. Therefore, it is plausible for the assumption (ii).

We now define the average network probe vehicle flow and density during time interval i on day d as follows

$$\bar{q}_p(d,i) = \frac{l_p(d,i)}{LT} = \frac{N_p(d,i) \cdot \bar{l}_p(d,i)}{LT} \tag{5a}$$

$$\bar{k}_p(d,i) = \frac{t_p(d,i)}{LT} = \frac{N_p(d,i) \cdot \bar{t}_p(d,i)}{LT} \tag{5b}$$

where $l_p(d,i)$ and $t_p(d,i)$ are total distance and time traveled by all probe vehicles in a road network during time interval i on day d, respectively.

Based on the abovementioned assumptions, we have the following relationship between the average flow (density) of probe vehicles and the average flow (density) of all vehicles:

$$\bar{q}_p(d,i) = \delta(i)\bar{q}(d,i) \tag{6a}$$

$$\bar{k}_p(d,i) = \delta(i)\bar{k}(d,i) \tag{6b}$$

The relationship implies that (i) if we could measure any two of $q_p(d,i)$, $\delta(i)$, and $\bar{q}(d,i)$, we will obtain the remaining one. (ii) if $\bar{q}(d,i)$ and $\bar{k}(d,i)$ are multi-day invariant, $\bar{q}_p(d,i)$ and $\bar{k}_p(d,i)$ will be multi-day invariant. Therefore, this is a day-to-day invariant MFD for probe vehicles; we simply call it pMFD.

3. Empirical observations

3.1. Data description
Beijing is the capital of China and one of the largest cities in the world. At the end of 2014, the number of taxi in Beijing reached 67,000 to meet the soaring travel demand from residents. The taxi has the characteristics of driving randomly, wide distribution, and the destination is determined by the passengers, which conform to the characteristics of residents' travel. In this paper, GPS-equipped taxi in urban area serves as probe vehicles to establish the pMFD. Every taxi uploads a set of instantaneous traffic information per minute, such as its positions, moving direction, speed, being occupied or not occupied by a passenger.
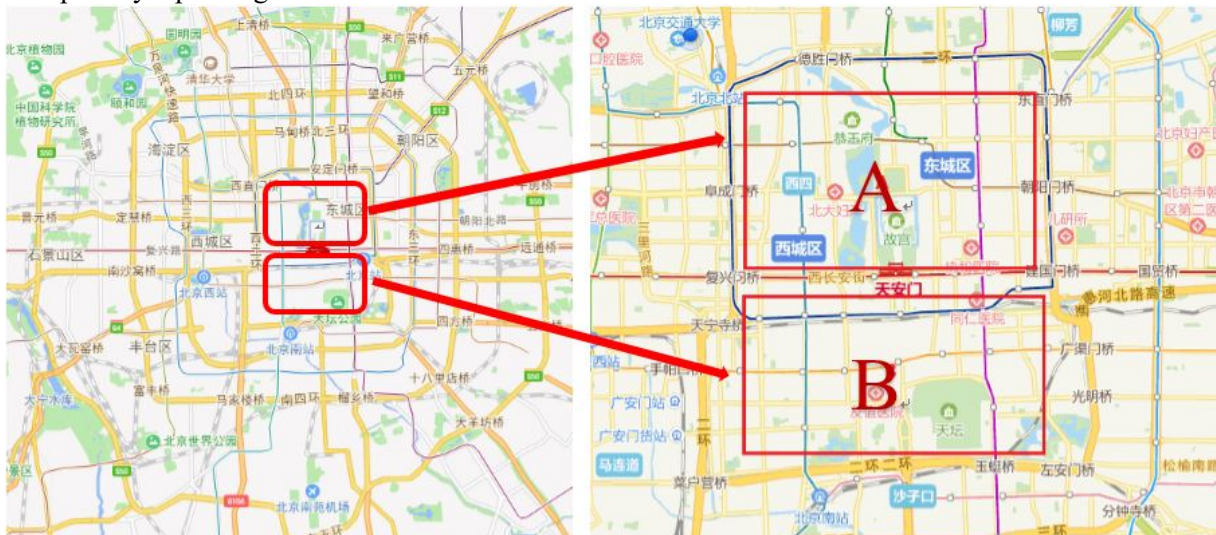

Figure 1. Two different region we choose in Beijing network.

To construct pMFD, we use the taxi data for 15 weekdays from 19th January to 6th February in 2015. Only the data beginning from 5 A.M. to 12 A.M. on weekdays are considered here, and the selected two regions within 2nd ring are presented in figure 1, where no freeway is included. Only the taxis that were occupied by passengers are considered here, because the behavior of these taxis is closer to that of regular vehicles.

3.2. Empirical observation of the day-to-day invariant pMFD
Set the time interval of aggregating probe vehicle data to be 5 min. Travel distance and travel time in every time interval is the straight-line distance and the time difference between two successive data points, respectively.

Figure 2 illustrates the empirical *p*MFD in region A on Jan. 22. It is obvious that the shape is not parabolic. Moreover, two distinguishing features (which will be carefully interpreted in the next section) can be observed: (i) The slope of the *p*MFD changes with traffic conditions, which might be caused by the changes of the traffic conditions in the empirical network. (ii) When VKT value reaches to maximum, the VKT and VHT decrease along the counter-clockwise loops. According to $\mathbf{VHT} = N_P \cdot \bar{t}_p$, when the congestion is dissipating, the number of occupied taxis N_P decreases and $\bar{l}_p$ increase. In the light of equation (6a), we conjecture the reason why $\bar{q}_p$ increase is that the penetration rate increases at this moment. As a result, if two points have the same VHT but different VKT (see points A and B), the point that appears earlier (point A) is lower than the point later (point B).
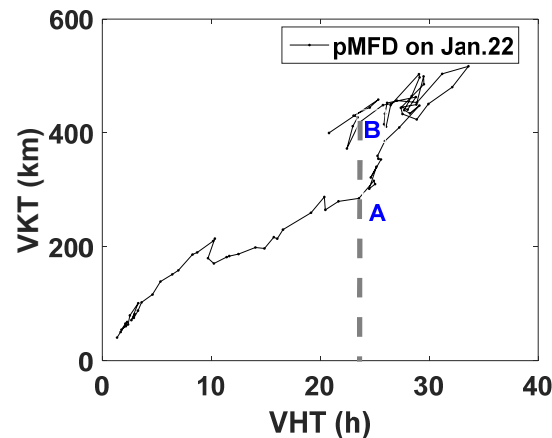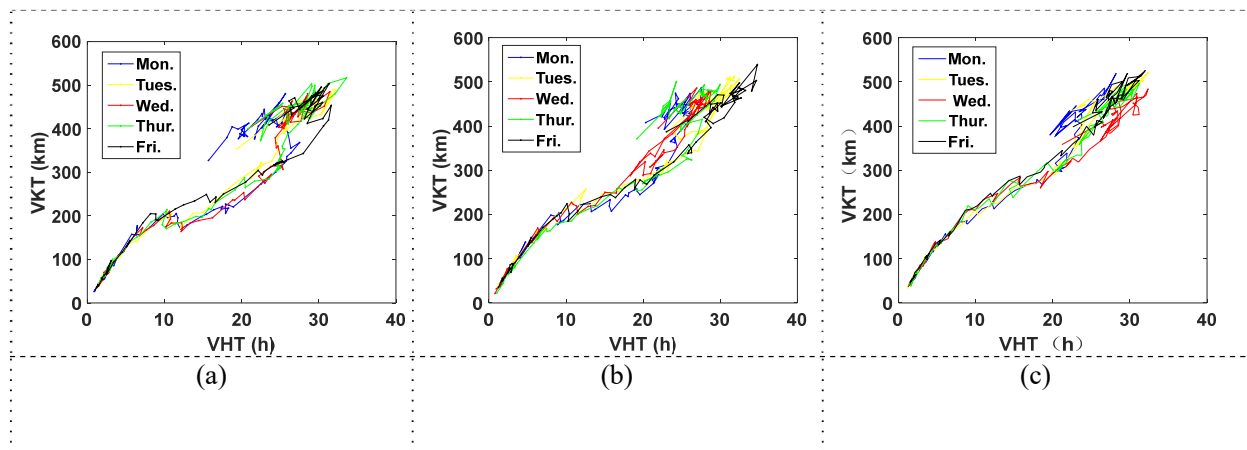

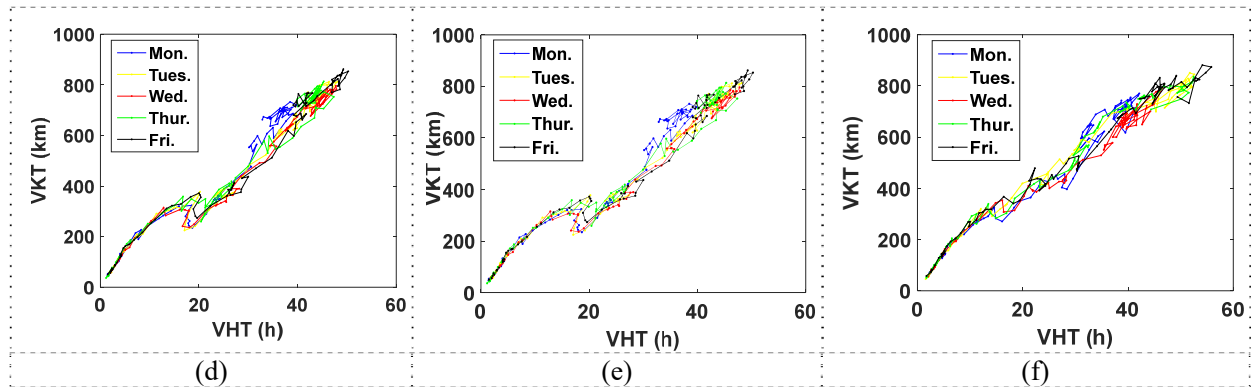Figure 2. The *p*MFD on Jan. 22 in region A.

| (a) | (b) | (c) |

Figure 3. Multi-day *p*MFD of two regions on three weeks (all workdays) using taxi trajectories. The region and week represented by each subfigure are: (a)region A, 1.19-1.23, (b)region A, 1.26-1.30, (c)region A, 2.2-2.6, (d)region B, 1.19-1.23, (e) region B, 1.26-1.30, (f) region B, 2.2-2.6.

Figure 3 shows multi-day *p*MFD on three weeks in two different regions. It can be seen that the shapes of the *p*MFD in the same region are similar and the difference among the maximum points is small, indicating that multi-day *p*MFD in a region is day-to-day invariant.

4. Interpretation of the shape of *p*MFD

4.1. Causes of pMFD's shape in Empirical Observation

Based on Edie's definition (Edie, 1965), the average network speed during time interval i on day d can be calculated as follows

$$\bar{v}(d,i) = \frac{\bar{q}(d,i)}{\bar{k}(d,i)} = \frac{\bar{l}(d,i)}{\bar{t}(d,i)} \tag{7}$$

According to Equations (5) and (6), we have

$$\bar{v}(d,i) = \bar{v}_P(d,i) = \frac{\bar{l}_p(d,i)}{\bar{t}_p(d,i)} \tag{8}$$

In accordance with equations (7) and (8), the average speed based on probe vehicles is equal to the average network speed of all vehicles. In light of relation between average network flow and density (see figure 4), the points at one time interval on the *p*MFD have the same slope to the points at the same time interval on the MFD, i.e., the points from different curves with the same slope have the same traffic condition.

Regarding the MFD, it can be seen from equation (1) that VKT and VHT are not only affected by the traffic condition, but also by the number of vehicles N. In contrast, the shape of the *p*MFD is additionally affected by the penetration rates of probe vehicles, i.e.,$\delta(i)$, according to equations (5) and (2).

We conjecture that in reality the variation of the penetration rate of the occupied taxis (i.e., the probe vehicle here) during a rush hour could be divided into three phases: Phase-1, before a rush hour: The total number of vehicles running in a network is relatively low, while the penetration rate of taxis is relatively high; Phase-2, during a rush hour: The total number of vehicles running in a network drastically increases and the penetration rate of taxis is relatively low; Phase-3, after a rush hour: The penetration rate of taxis increases along with the decrease of the total number of vehicles. In the following subsection, we will show in a simulation scenario that the variation of penetration rates is the main cause.
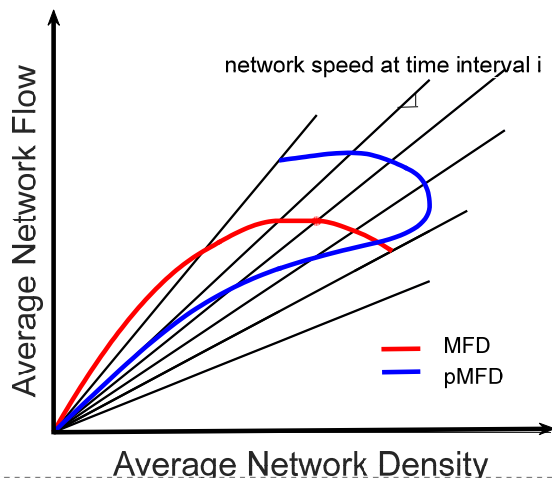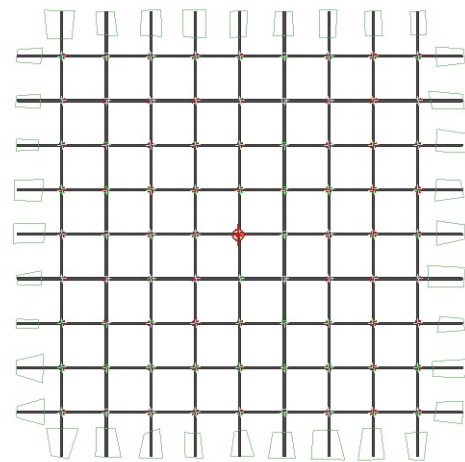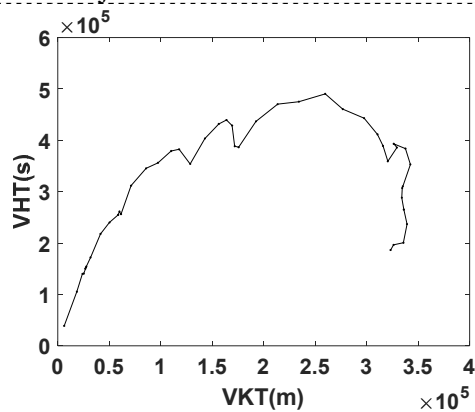
Figure 4. A schematic diagram to compare *p*MFD and MFD.

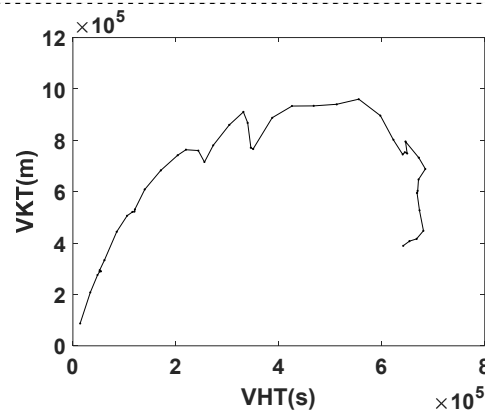

Figure 5. An idealized simulation network

4.2. Simulation test

This subsection tests the impact of the penetration rate of probe vehicles on the shape of the *p*MFD in a simulation scenario built in Paramics, a microscopic traffic simulations software.

The scenario contains a 9×9 square grid network with 4-lane two-way, where there are 216 links and each link is 300 meters. For simplicity, all traffic zones are placed at the ends of all peripheral links, resulting in a total of 36 traffic zones (see figure 5). A random symmetric origin-destination matrix is set as initial demand in a warm-up period. Then, the demand is increased until the simulation network is jammed.
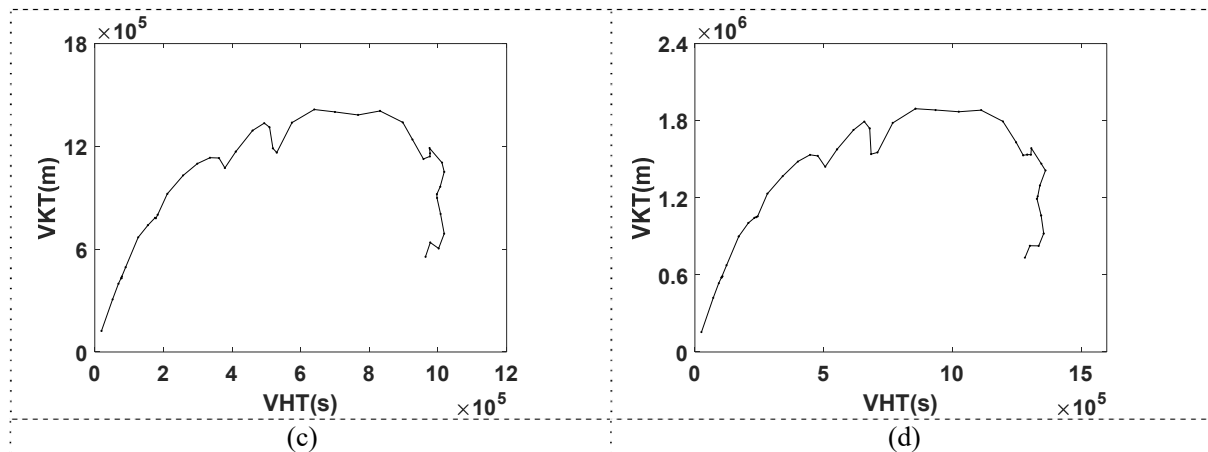

(a)

(b)

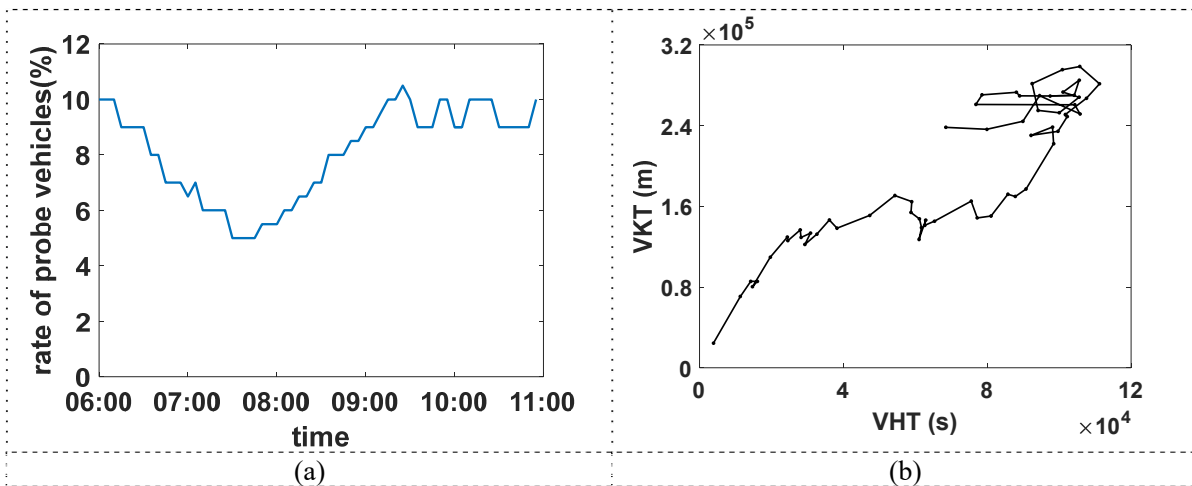Figure 6. MFD in idealized simulation network used (a) 20%, (b) 40%, (c) 60% and (d) 80% probe vehicle data.

Figure 7. (a) Time-varying demands and (b) Simulated pMFD.

The pMFD associated with the simulated network is plotted in figure 6, where the penetration rates of probe vehicles (i.e.,$\delta(i)$) are set to be 20%, 40%, 60% and 80%. It can be seen that the points gather along a smooth parabolic curve, indicating that a well-defined with low-scatter pMFD exists by using probe vehicles data when the penetration rate doesn't change.
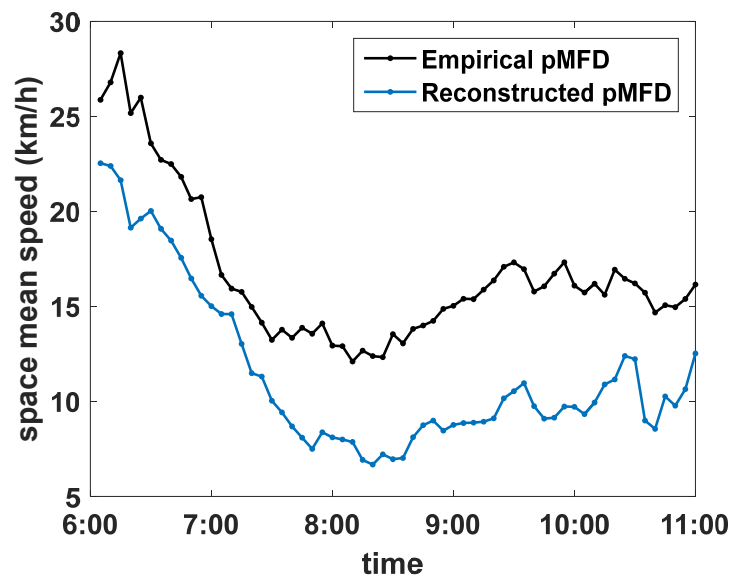
Figure 8. Comparison of VHT between the empirical *p*MFD and the simulated *p*MFD

Subsequently, we dynamically change the penetration rates of probe vehicles following the demands given in figure 7a, from which three periods abovementioned can be seen. Figure 7b shows the resulting *p*MFD. It can be seen that the shape of the simulated *p*MFD in figure 7b is consistent with that of the empirical *p*MFD shown in figure 2. Figure 8 further compares the simulated and empirical *p*MFD in a time-series manner, which further enhances our observation about the consistency. Therefore, it is shown through the simulation test that our previous conjecture, i.e., the shape of the *p*MFD is impacted by the dynamical changes of the penetration rates of probe vehicles, is reasonable.

5. Conclusion

This paper proposes a day-to-day invariant MFD for probe vehicles, called *p*MFD. It is directly and simply constructed by using probe vehicle data. By using multi-day taxi data, it is demonstrated that the shape of the *p*MFD is day-to-day invariant, which is a very valuable property as a MFD. In a simulation scenario, the shape shown in the empirical *p*MFD is explained; i.e., it is attributed to the time-varying changes of the penetration rate of probe vehicles. Due to the wide existence of the probe vehicle data, the *p*MFD is potential to be a type of MFD that deserves carefully studies about its characteristics and related traffic control strategies.

Acknowledgement

References
[1] N. Geroliminis and C. F. Daganzo, "Existence of urban-scale macroscopic fundamental diagrams: Some experimental findings," Transportation Research Part B: Methodological, vol. 42, no. 9, pp. 759 – 770, 2008.

[2] C. Buisson and C. Ladier, "Exploring the impact of homogeneity of traffic measurements on the existence of macroscopic fundamental diagrams," Transportation Research Record Journal of the Transportation Research Board, vol. 137, no. 2124, pp. 127–136, 2009.

[3] N. Geroliminis and J. Sun, "Hysteresis phenomena of a macroscopic fundamental diagram in freeway networks," Transportation Research Part A, vol. 45, no. 9, pp. 966–979, 2011.

[4]   A. S. Nagle and V. V. Gayah, "Accuracy of networkwide traffic states estimated from mobile probe data," Transportation Research Record Journal of the Transportation Research Board, vol. 2421, no. 2421, pp.1–11, 2014.

[5]   M. Saberi and H. S. Mahmassani, "Hysteresis and capacity drop phenomena in freeway networks: empirical characterization and interpretation," Transportation Research Board Annual Meeting, 2013.

[6]   T. Tsubota, A. Bhaskar, and E. Chung, "Macroscopic fundamental diagram for brisbane, australia empirical findings on network partitioning and incident detection," Transportation Research Record Journal of the Transportation Research Board, vol. 2421, no. 2421, pp. 12–21, 2014.

[7]   Z. He, S. He, and W. Guan, "A figure-eight hysteresis pattern in macroscopic fundamental diagrams and its microscopic causes," Transportation Letters, vol. 7, no. 3, pp. 133–142, 2014.

[8]   J. Haddad and N. Geroliminis, "On the stability of traffic perimeter control in two-region urban cities," Transportation Research Part B, vol. 46, no. 9, pp. 1159–1176, 2012.

[9]   N. Zheng, R. A. Waraich, K. W. Axhausen, and N. Geroliminis, "dynamic cordon pricing scheme combining the macroscopic fundamental diagram and an agent-based traffic model," Transportation Research Part A Policy & Practice, vol. 46, no. 8, pp. 1291–1303, 2012.

[10] M. Keyvan-Ekbatani, A. Kouvelas, I. Papamichail, and M. Papageorgiou,"Exploiting the fundamental diagram of urban networks for feedback based gating," Transportation Research Part B: Methodological,vol. 46, no. 10, pp. 1393 – 1403, 2012.

[11] M. Ramezani, J. Haddad, and N. Geroliminis, "Dynamics of heterogeneity in urban networks: aggregated traffic modeling and hierarchical control," Transportation Research Part B, vol. 74, pp. 1–19, 2015.

[12] J. Haddad and B. Mirkin, "Adaptive perimeter traffic control of urban road networks based on mfd model with time delays," International Journal of Robust & Nonlinear Control, vol. 26, no. 6, pp. 1267–1285,2016.

[13] G. Mariotte, L. Leclercq, and J. A. Laval, "Macroscopic urban dynamics: Analytical and numerical comparisons of existing models," Transportation Research Part B Methodological, vol. 101, p. 245267, 2017.

[14] v. Z. H. S. L. 10. Beibei, J., "Determining the macroscopic fundamental diagram on the basis of mixed and incomplete traffic data," Transportation Research Board Annual Meeting, 2016.

[15] L. Ambhl and M. Menendez, "Data fusion algorithm for macroscopic fundamental diagram estimation," Transportation Research Part C Emerging Technologies, vol. 71, pp. 184–197, 2016.

[16] J. Du, H. Rakha, and V. V. Gayah, "Deriving macroscopic fundamental diagrams from probe data: Issues and proposed solutions," Transportation Research Part C Emerging Technologies, vol. 66, pp. 136–149, 2016.

[17] L. C. Edie, "Discussion of traffic stream measurements and definitions,"1965.